JOURNAL OF APPLIED CRYSTALLOGRAPHY
ISSN 1600-5767

XMDYN and *XATOM*: versatile simulation tools for quantitative modeling of X-ray free-electron laser induced dynamics of matter[1]

Zoltan Jurek,[a,b]* Sang-Kil Son,[a,b] Beata Ziaja[a,b,c] and Robin Santra[a,b,d]

[a]Center for Free-Electron Laser Science, DESY, Notkestrasse 85, 22607 Hamburg, Germany, [b]The Hamburg Centre for Ultrafast Imaging, Luruper Chaussee 149, 22761 Hamburg, Germany, [c]Institute of Nuclear Physics, Polish Academy of Sciences, Radzikowskiego 152, 31-342 Kraków, Poland, and [d]Department of Physics, University of Hamburg, Jungiusstrasse 9, 20355 Hamburg, Germany. *Correspondence e-mail: zoltan.jurek@desy.de

Received 20 January 2016
Accepted 11 April 2016

Edited by Ne-Te Duane Loh, National University of Singapore Centre for Bioimaging Sciences

[1] This article will form part of a virtual special issue of the journal on free-electron laser software.

Keywords: X-ray free-electron lasers; XFELs; dynamics of matter; ionization dynamics; radiation damage; computer programs.

Rapid development of X-ray free-electron laser (XFEL) science has taken place in recent years owing to the consecutive launch of large-scale XFEL instruments around the world. Research areas such as warm dense matter physics and coherent X-ray imaging take advantage of the unprecedentedly high intensities of XFELs. A single XFEL pulse can induce very complex dynamics within matter initiated by core-hole photoionization. Owing to this complexity, theoretical modeling revealing details of the excitation and relaxation of irradiated matter is important for the correct interpretation of the measurements and for proposing new experiments. *XMDYN* is a computer simulation tool developed for modeling dynamics of matter induced by high-intensity X-rays. It utilizes atomic data calculated by the *ab initio XATOM* toolkit. Here these tools are discussed in detail.

1. Introduction

X-ray free-electron lasers (XFELs) (Ackermann *et al.*, 2007; Emma *et al.*, 2010; Ishikawa *et al.*, 2012) produce intense radiation with a pulse duration of only tens of femtoseconds or less and with an intensity many orders of magnitude higher than what one can obtain with storage-ring-based synchrotron radiation sources. Although the cross sections for the elementary processes following X-ray–matter interaction are typically small, the high fluence delivered within a single shot increases ionization probabilities to saturation. Various photoinduced processes are in competition with each other, even within an isolated atom. Highly nonlinear phenomena emerge because of the complex ionization pathways within the molecular environment.

As a consequence, all areas of research exploiting intense X-ray pulses, such as warm dense matter, nanocrystallography and coherent diffraction imaging, require a thorough understanding of the unavoidable ionization processes following X-ray irradiation. Theoretical models and accurate simulation tools are needed to predict the behavior of irradiated matter. Numerical modeling of plasmas created by optical irradiation of rare gas clusters, including microscopic processes, was initiated in the 1990s by Ditmire (1998). Since the X-ray free-electron laser facilities have been in operation, great effort has been put into the development of computational tools to model soft and hard X-ray irradiation of matter (*e.g.* Siedschlag & Rost, 2002; Jurek *et al.*, 2004; Hau-Riege *et al.*, 2004; Jungreuthmayer *et al.*, 2004; Ziaja *et al.*, 2006; Gnodtke *et al.*, 2011; Peltz *et al.*, 2012; Hau-Riege *et al.*, 2013). All these tools use classical mechanics to propagate the system in real space.

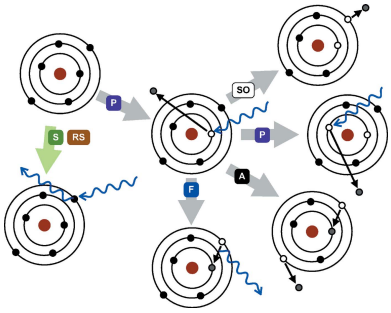

Here we report on our approach primarily designed for the hard X-ray case, which has resulted in two codes, *XMDYN* (Jurek *et al.*, 2013) and *XATOM* (Son & Santra, 2011). Executables of both codes are available *via XRAYPAC* (Jurek *et al.*, 2016). They have been successfully used to quantitatively interpret experiments. *XMDYN* is a molecular-dynamics-based particle code to simulate ionization dynamics within irradiated finite-size molecular assemblies. *XATOM* is an *ab initio* code based on the Hartree–Fock–Slater approach. It can calculate orbital energy levels, rates of photoinduced processes, and ionization dynamics in neutral atoms and atomic ions. The on-the-fly communication between these tools enables us to perform simulations without calculating in advance atomic data and, therefore, to explore any molecular assemblies consisting of any types of atomic species.

The paper is structured as follows. First we give an overview of the *XATOM* tool. This is followed by a description of *XMDYN*, in particular, of the theoretical model applied and of the code structure used in published work, with the focus on the high-intensity irradiation regime. Finally, we list the technical details needed for code implementation and provide a simplified manual.

2. *XATOM*

2.1. Overview

XATOM is an integrated toolkit for X-ray atomic physics. It provides a theoretical description of fundamental X-ray–atom interactions. In particular, *XATOM* is designed for describing complex interactions between atoms and intense XFEL pulses. During the XFEL–atom interaction, if single-photon absorption is saturated, multiphoton absorption occurs *via* a sequence of single-photon ionization and accompanying relaxation processes like fluorescence and Auger decay. The X-ray multiphoton absorption usually yields highly charged states, involving a variety of different multiple-hole states. *XATOM* calculates atomic data – orbitals and orbital energies, and cross sections and rates for X-ray-induced processes – for all individual electronic configurations, including multiple-hole states, of arbitrary atomic species. These atomic data are used not only for simulating ionization dynamics of atoms within *XATOM* but also as input for *XMDYN* simulations for complex systems. The current version of *XATOM* can calculate the following X-ray-induced atomic processes (see Fig. 1):

(1) photoionization cross section,
(2) X-ray fluorescence rate,
(3) Auger (Coster–Kronig) decay rate,
(4) elastic X-ray scattering cross section and its dispersion correction (Son, Chapman & Santra, 2011),
(5) Compton scattering cross section (Slowik *et al.*, 2014),
(6) shake-off branching ratio (Doumy *et al.*, 2011).

The theoretical background of *XATOM* is given by Santra (2009), the implementation of *XATOM* is described by Son, Young & Santra (2011), and Santra & Young (2014) provide a review of many *XATOM* applications.

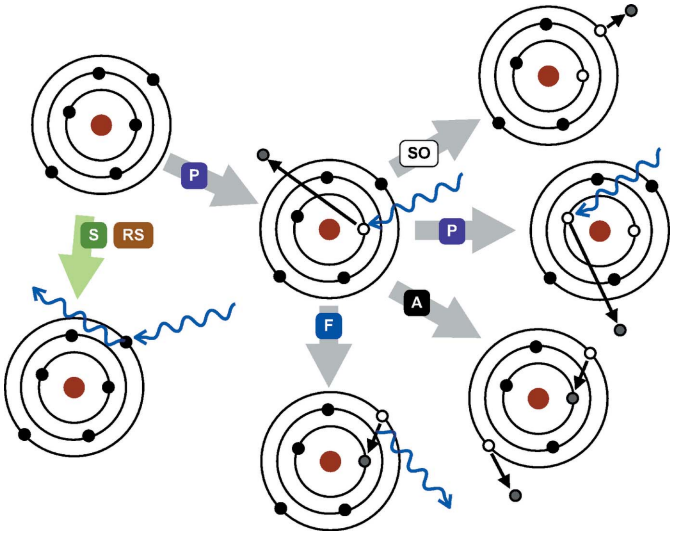

Figure 1
Diagrams of X-ray-induced physical processes treated by *XATOM*. P: photoionization; A: Auger (Coster–Kronig) decay; F: fluorescence; SO: shake-off; S: Rayleigh and Compton X-ray scattering; RS: resonant elastic X-ray scattering.

2.2. Numerical procedure

In *XATOM*, the electronic structure is treated quantum mechanically. The effective single-electron Schödinger equation to be solved is

$$\left[-\tfrac{1}{2}\nabla^2 + V(\mathbf{r})\right]\psi(\mathbf{r}) = \varepsilon\psi(\mathbf{r}), \tag{1}$$

where ψ is an atomic orbital and ε is the corresponding orbital energy. We use the Hartree–Fock–Slater (HFS) method (Slater, 1951), which employs a local density approximation to the exact exchange interaction. The potential is then given by

$$V(\mathbf{r}) = -\frac{Z}{r} + \int \mathrm{d}^3 r' \, \frac{\rho(\mathbf{r}')}{|\mathbf{r}-\mathbf{r}'|} - \frac{3}{2}\left[\frac{3}{\pi}\rho(\mathbf{r})\right]^{1/3}, \tag{2}$$

where Z is the nuclear charge of the given atom. The electron density $\rho(\mathbf{r})$ is assumed to be spherically symmetric, and the spin polarization is averaged. For the atomic system, the electronic configuration is given by the set of occupation numbers of the (n, l) subshells, where n is the principal quantum number and l is the orbital angular momentum quantum number. Using the HFS method, the multiple-hole states are calculated for the corresponding electronic configuration. The orbitals are re-optimized for every single electronic configuration that may be formed by removing zero, one or more electrons from the ground-state configuration of the neutral atom.

X-ray-induced atomic processes are treated in a consistent *ab initio* theoretical framework, based on nonrelativistic quantum electrodynamics and perturbation theory. The cross sections and rates are calculated with transition matrix elements involving bound wavefunctions as well as continuum wavefunctions. The bound wavefunctions are expressed by a numerical radial function and analytical spherical harmonics; the former is accurately solved by the pseudospectral method on a non-uniform radial grid (Yao & Chu, 1993; Tong & Chu,

1997). For the continuum wavefunctions, we use the same potential as used for the bound wavefunctions, so orthogonality between bound and continuum wavefunctions is preserved. The continuum wavefunctions for given positive energies are numerically solved by the fourth-order Runge–Kutta method on a uniform radial grid.

To describe X-ray multiphoton ionization dynamics, we employ a rate-equation model (Rohringer & Santra, 2007; Makris *et al.*, 2009; Young *et al.*, 2010). The calculated cross sections and rates serve as input parameters for a set of coupled rate equations for the time-dependent configurational populations, which can be solved within the *XATOM* package for the atomic case. The coupled rate equations are solved by (i) direct time propagation (Son, Young & Santra, 2011), (ii) a Monte Carlo approach with a pre-calculated table of atomic data (Rudek *et al.*, 2012; Son & Santra, 2012) or (iii) Monte Carlo on the fly (Fukuzawa *et al.*, 2013). In the last approach, ionization pathways are chosen by a Monte Carlo scheme and atomic data are calculated only when the corresponding electronic configuration is visited on the ionization pathway. To treat X-ray multiphoton ionization dynamics for complex systems, *XMDYN* employs the atomic data calculated by *XATOM*. In *XMDYN*, ionization dynamics of bound electrons are treated by a Monte Carlo approach, which will be explained in §3.2.2. Note that the *XATOM* toolkit has been extended to the atoms embedded in a plasma environment (Thiele *et al.*, 2012; Son *et al.*, 2014). Also, recently, the atomic orbitals optimized for core-hole states have been used as basis functions for molecular electronic structure calculations of multiple-hole states (Hao *et al.*, 2015).

2.3. Applications: X-ray multiphoton ionization of atoms and X-ray molecular imaging

The sequential X-ray multiphoton ionization dynamics model has been tested with a series of gas-phase atomic experiments conducted at the Linac Coherent Light Source (LCLS) (Doumy *et al.*, 2011; Rudek *et al.*, 2012, 2013) and at SACLA (Fukuzawa *et al.*, 2013; Motomura *et al.*, 2013). After solving rate equations within *XATOM*, one can generate ion spectra, electron spectra and photon spectra (Son & Santra, 2012), which may be directly compared with experimental results after integrating over the interaction volume (Young *et al.*, 2010; Rudek *et al.*, 2012).

XATOM is used to investigate scattering patterns including electronic radiation damage (Son, Young & Santra, 2011). Detailed understanding of electronic damage dynamics is critical in serial femtosecond crystallography, for example, because the scattering strength dramatically changes as a result of the huge amount of ionization during an intense X-ray pulse. This electronic damage is particularly severe for heavy atoms because of their large photoionization cross section. According to our understanding of the dynamical behavior of atoms during the pulse, the extensive ionization of heavy atoms becomes beneficial for molecular imaging, especially for addressing the phase problem. We proposed a new high-intensity formulation of the multiwavelength anomalous diffraction method (Son, Chapman & Santra, 2011; Son *et al.*, 2013), which is applicable for phasing in femtosecond nanocrystallography. Utilizing the selective and extensive ionization of heavy atoms, we further developed high-intensity phasing techniques (Galli, Son, White *et al.*, 2015; Galli, Son, Klinge *et al.*, 2015; Galli, Son, Barends *et al.*, 2015). So far, the ionization dynamics model used in the above X-ray imaging applications has been based on the independent atom model without a molecular or plasma environment. *XMDYN* combined with *XATOM* will be able to achieve realistic simulations of radiation damage dynamics and is expected to play a key role in X-ray molecular imaging and novel phasing methods.

3. *XMDYN*

3.1. Overview

XMDYN is a computational tool to simulate dynamics of matter exposed to high-intensity X-rays. The foundations of this hybrid atomistic approach were described by Jurek *et al.* (2004). Neutral atoms, atomic ions (later referred to as ions) and ionized (free) electrons are treated as classical particles, with defined position and velocity vectors, charge, and mass. The molecular dynamics (MD) technique is applied to calculate their real-space dynamics. Electronic configurations of atoms and ions are followed by tracking the occupation of the orbitals using a Monte Carlo algorithm. Related parameters such as orbital binding energies are calculated with *XATOM*.

A log file contains all ionization events that have occurred during the time evolution. Microscopic data of the individual atoms and electrons are saved in snapshots. These time-resolved data can be used for theoretical studies either directly (*e.g.* in ion or electron spectroscopy) or as input (*e.g.* in X-ray imaging).

3.2. Numerical procedure

3.2.1. Program structure. The program starts with loading the input. This is followed by a time evolution loop (Fig. 2). In the simplest single-timestep scheme the system is propagated within the time loop, using a small finite timestep, DT (typically DT $\lesssim$ attosecond). Within one cycle of the time loop major blocks are being executed as a sequence. The evaluation of photoionization and Auger and fluorescent relaxation is performed within the Monte Carlo block (MC-block), and the real-space propagation of the classical particles in the Molecular Dynamics block (MD-block). Checking for secondary ionization (electron impact ionization) and electron–ion recombination occurs in the Collision block (CO-block) and Recombination block (RE-block), respectively.

DT should be chosen in such a way that it fits the timestep requirements of each block. At the same time, it should be short enough that the blocks can be evaluated independently in a sequence within one cycle of the time loop. The MC-block is 'insensitive' to the choice of DT, and the timescales of the CO-block are directly connected to the real-space dynamics (see details of these blocks later). Therefore, DT is basically

determined by the energy conservation requirements of the MD-block only.

Whenever a new atomic configuration appears during a run, an atomic data list is loaded. The atomic data list primarily contains data needed for the simulation of the dynamics, such as orbital binding energies and a list of atomic processes (photoionization, Auger decay *etc.*) that can occur with their corresponding cross section or rate values. The atomic data list may contain other data such as atomic form factors or inelastic X-ray scattering cross sections if the option is set in the input file. In the general case the data are calculated on the fly *via* an automatic call of *XATOM* or are loaded from files of precalculated tables.

3.2.2. MC-block. *XMDYN* loads the process lists for the atoms/ions (after start) and updates them whenever configurations change, *e.g.* during ionization events. The atomic data are kept in a tree-structured database sorted according to the orbital occupation. Actual data are assigned to an atom by using pointers (Fig. 3). In this way all data are loaded only once during a run and multiple storage of data is avoided. Specific data can be loaded from a file named after the corresponding electronic configuration (*e.g.* `1s2_2s0_2p2.dat`), which contains a table of the atomic parameters precalculated with *XATOM*. If no such file is available, *XMDYN* calls *XATOM* directly and reads the data on the fly through a Unix process pipe.

Photoionization and the inner-shell Auger and fluorescent decays are purely stochastic processes within *XMDYN*. The MC-block generates an ionization pathway (a sequence of electronic configurations) of the individual atoms and ions for a time interval DT, using a Monte Carlo scheme. The scheme requires no predefined micro timestep to handle elementary processes, which may have characteristic timescales spread over many orders of magnitudes.

The following algorithm is used:

(1) Determine the w_{i_α} rates of i_α elementary processes for all α atoms/ions. In the case of the Auger and fluorescent decays the rates are directly calculated with *XATOM*. For photoionization, $w_{i_\alpha} = \sigma_{i_\alpha} I\,\mathrm{DT}$, where σ_{i_α} is the cross section of the process (calculated with *XATOM*) and I is the X-ray flux, assumed constant during the short time interval DT.

(2) The elementary processes follow an exponential decay law. According to this, choose random times $t_{i_\alpha} = -\ln(\xi_{i_\alpha})/w_{i_\alpha}$ for all processes, where $\{\xi_{i_\alpha}\}$ are random numbers of uniform distribution in the interval (0, 1) generated by the random number generator of the computer. In what follows we will refer to the smallest time as t_{j_β}.

(3) Interpret the above t_{i_α} numbers. If all t_{i_α} times were larger than DT, no event has occurred during DT and the MC-block finishes in the current cycle of the time loop. Otherwise, an event j_β of atom β has occurred at the time t_{j_β}, but no other

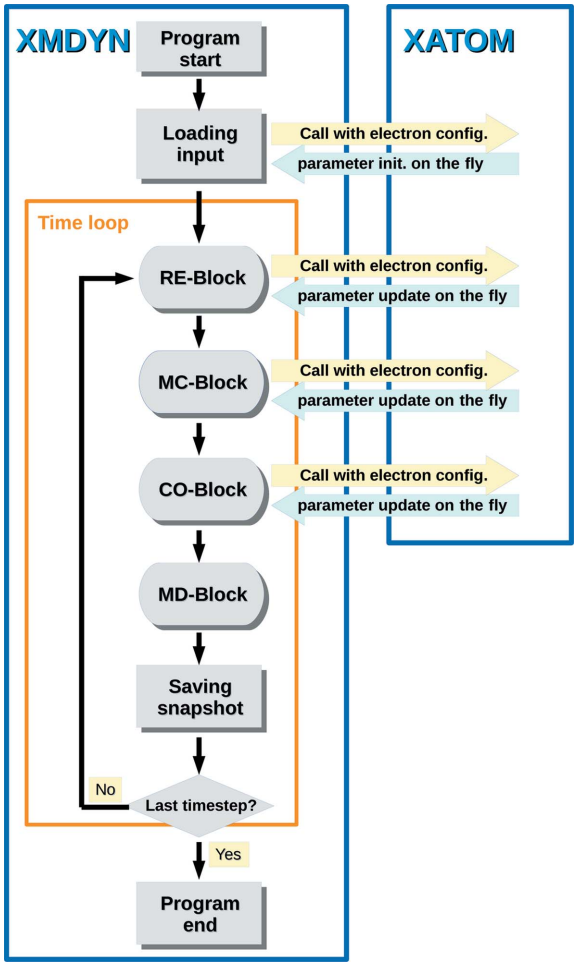

Figure 2
Flowchart of *XMDYN* showing the internal structure of the main blocks responsible for the evaluation of various processes. At program start and whenever the electronic configuration of an atom/ion changes, atomic parameters are loaded from files by calling *XATOM* on the fly.

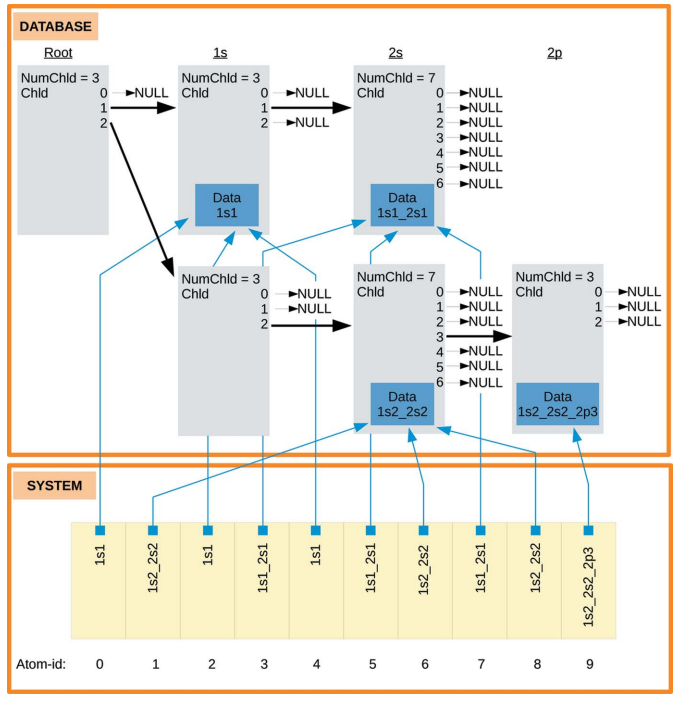

Figure 3
The loaded atomic data are organized in a tree-structured database. The data are assigned to the atoms and ions, using pointers. The figure depicts an example for a system of ten ions.

event has occurred within the $[0, t_{j_\beta}]$ interval. The electronic configuration of atom β is changed according to process j_β and the list of its possible processes (containing the corresponding atomic parameters) is updated correspondingly.

(4) Go back to step 1. In the next cycle steps 1–3 are executed for the shorter DT $- t_{j_\beta}$ period.

Owing to the different treatment of the bound and free electrons there is a necessary bound–free transition enforced during an ionization event: a new classical electron is placed in the vicinity of the ion. It satisfies the corresponding energy and momentum conservations. For example, in the case of photoionization the total classical energy and momentum of the system are changed by $E_{\rm photon} - E_{\rm binding}$ (the asymptotic kinetic energy of the electron) and $E_{\rm photon}/c$ (c being the speed of light), respectively. This requires the algorithm to change the velocity of the affected ion and to set the velocity of the newly created classical electron. To determine these values, first the direction of the velocity of the ejected electron is fixed, according to the corresponding angular distribution. Then, the electron is placed at a predefined small distance from the ion in the direction parallel to the electron velocity (radial ejection). Finally, four scalar conservation equations for three momenta + energy are solved to determine the magnitude of the electron velocity and three components of ion velocity. During Auger decay the same procedure is applied, but the Auger electron energy increments the classical energy of the system while the total momentum remains constant.

3.2.3. MD-block. The real-space dynamics of the classical particles (atoms, ions and electrons released during ionization) are governed by the Newton equations $m_i\,{\rm d}^2\mathbf{r}_i/{\rm d}t^2 = \mathbf{F}_i$, which are integrated numerically. Since the maximal electron kinetic energies can be expected to be of the order of the photon energy, a nonrelativistic treatment is justified in the X-ray regime. During irradiation with a high-fluence X-ray pulse the ionization progresses fast, chemical bonds disappear quickly and the predominant forces driving the dynamics are due to Coulomb interaction between the generated charges. We use a pair potential of the form $q_1q_2/(r^2 + r_0^2)^{1/2}$ introduced in MD plasma modeling by Ditmire (1998). Assuming a finite value of r_0 (defined in the input file), we avoid numerical instability caused by the singularity at the zero distance. We fix the value of r_0 during simulations. Typically, r_0 is around 0.5–1 Å. It is often adjusted in such a way that the well depth is close to the smallest binding energy of the neutral atom. In the simplest case the propagation is done by the widely used (single timestep) velocity Verlet algorithm (Swope *et al.*, 1982). The accuracy of energy conservation is tracked and used to monitor how much the error of the numerical integration accumulates.

In most cases the MD-block is the computationally most expensive block during a single run because the number of interparticle forces scales with N^2 for a system of N particles. Within the MD framework, we use special strategies to speed up the calculations. A straightforward route is parallelization, in particular, by using dedicated hardware. *XMDYN* has an extension to evaluate Coulomb and van der Waals forces on graphical processing units (GPUs) based on the Chamomile scheme (Hamada & Iitaka, 2007). A single GPU card can yield a performance equal to hundreds of CPU cores. While a GPU can be efficient for a large number of particles, another strategy is needed when the system is small. For such a situation we implemented the multiple timestep position Verlet scheme discussed by Qian & Schlick (2002) and Barash *et al.* (2003), which yielded ∼30–50 times speedup in our applications. In this case, the timestep DT is chosen to be large and it is split into sub-steps within the algorithm (Fig. 4). Our

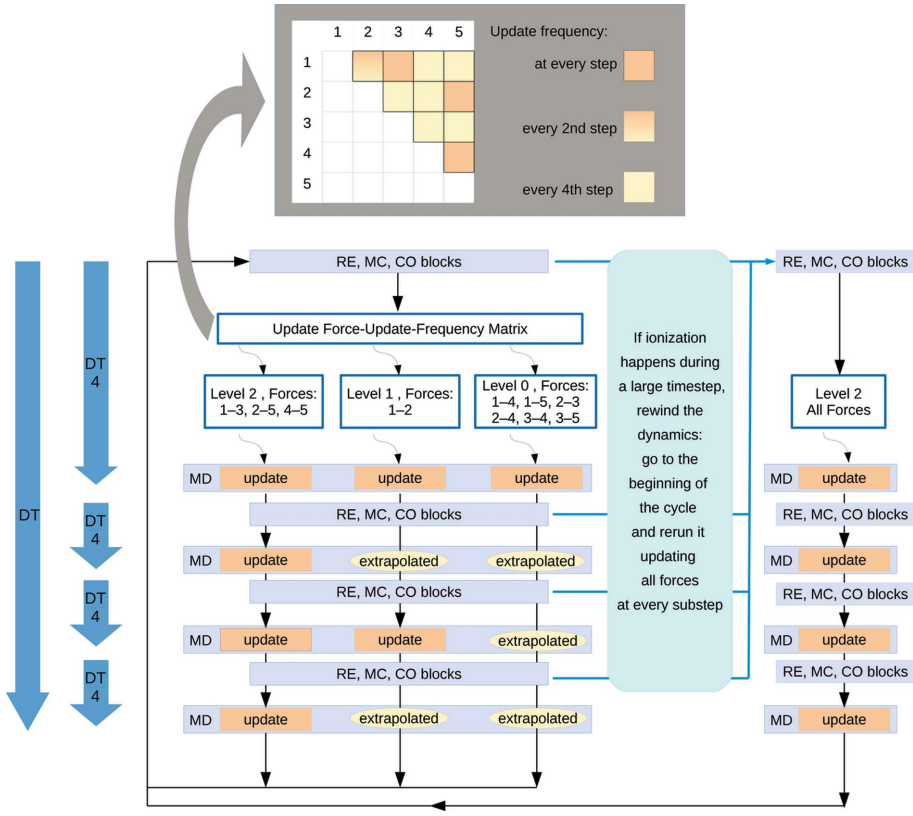

Figure 4
The multiple timestep scheme implemented within *XMDYN*. In the current example it is shown for $n = 2$ with the evaluation levels 0, 1, 2 and 2^n sub-timesteps. At the beginning of a cycle covering a 'large' timestep DT all particle pairs are examined and classified on the basis of their mutual distance, which reflects how fast their interaction is expected to change (interaction matrix with colors). According to the classification some forces are evaluated less frequently and, instead, extrapolated for forthcoming sub-steps. Note that, whenever an ionization happens during a cycle, all particle data are restored to their value at the beginning of that cycle and the dynamics for the time interval DT are recalculated by evaluating all forces with the highest frequency.

implementation extends the algorithm of Qian & Schlick (2002) and Barash *et al.* (2003) with the possibility of defining n different update levels when applying 2^n substeps. At the beginning of each DT cycle, particle pairs are classified on the basis of how fast the force between them is expected to vary (matrix with colors in example Fig. 4). In the case of fast force change, the forces are evaluated frequently, even at every sub-timestep. Slowly varying forces are calculated less frequently. At the time of their evaluation they are extrapolated to be used at the forthcoming sub-timesteps. The classification is based on interparticle distances, *e.g.* electron–electron forces are evaluated more frequently below a critical distance, while less frequently above it. A specific choice of distance parameters is verified by proper energy conservation in test runs. Note that the extrapolation-based multiple timestep scheme works if the system remains conservative during the large timestep, DT, *e.g.* if potentials do not change suddenly. As this criterion is not fulfilled when an ionization event occurs during the time interval DT, time evolution is then recalculated, applying the largest update frequency for all pairs during that cycle. For small systems and long time propagations the number of such repetitions is small within the whole propagation. Therefore, the strategy yields overall a significant speedup.

3.2.4. CO-block. In our model collisional (electron impact) ionization is not a stochastic process but deterministic. It depends on the spatial location of the particles: the impact electron has to be in the vicinity of the target atom. *XMDYN* utilizes a procedure based on the treatment discussed by Jurek *et al.* (2004). When a classical electron is closest to an atom/ion, its trajectory is extrapolated back to infinite distance in the potential of the target ion by using energy and angular momentum conservation. Collisional ionization occurs when the impact parameter at infinity is smaller than the radius associated with the total electron impact ionization cross section. The total cross section is a sum of partial cross sections evaluated for the occupied orbitals, using the asymptotic kinetic energy of the impact electron. In the case of an ionization event the orbital to be ionized is chosen randomly, using the probability distribution obtained with the subshell cross sections. In the current implementation the atomic binary-encounter-Bethe (BEB) (Kim & Rudd, 1994) cross sections are used. The required atomic parameters are taken from *XATOM*.

3.2.5. RE-block. In a classical particle model classical electron capture may occur. It is due to three-body (or many-body) recombination, which is the main recombination channel in a dense charged environment. The code regularly checks for the ions that produce the strongest Coulomb potential for each electron and tracks how long this condition holds. When the electron stays for n full periods around the same ion (the small integer n being an input parameter) the system is identified as recombined (similarly to Georgescu *et al.*, 2007). In practice, this procedure is done by projecting the trajectory around the ion to the (x, y) laboratory-frame plane and by accumulating the angular motion centered around the projected ion. The plane chosen for this analysis can be arbitrary, as the projection of a three-dimensional motion confined around an ion to any plane is also a confined two-dimensional trajectory. The exceptional 'ill case', where an orbit is perfectly perpendicular to the plane chosen, cannot remain stable within an interacting environment. In order to be consistent with the hybrid approach (see §3.1) the electron is kept classical if its classical orbital energy is higher than the orbital energy of the highest considered orbital i containing a vacancy. When the classical binding becomes stronger, the classical electron is removed and the occupation number of orbital i is incremented by one. The information about the classically recombined electron–ion subsytems is also saved in the snapshot files. In the applications listed in §3.3, recombination was identified during postprocessing based on the saved snapshots. Now *XMDYN* identifies it internally during the run and logs these recombination events within the RE-block.

3.3. Applications: spectroscopy and X-ray imaging

A straightforward area of applications for *XMDYN* is the interpretation of data from spectroscopy experiments. These observables are directly connected to the dynamics of the sample. Therefore, they can also be used to validate the model.

Spectroscopy on gas-phase C_{60} molecules was performed at the LCLS. The *XMDYN* results showed good quantitative agreement with the measured ion data. The simulations allowed us to get more insight into the femtosecond explosion of the fullerenes (Murphy *et al.*, 2014). Another spectroscopy experiment quantitatively described by *XMDYN* was the experiment by Tachibana *et al.* (2015) performed at SACLA to study nanoplasma formation. In this experiment, rare gas (Ar and Xe) atom clusters were irradiated by hard X-ray laser pulses and their electron kinetic energy spectra were measured. Simulations with *XMDYN* confirmed the nanoplasma formation and provided a detailed understanding of the specific ionization mechanisms. The study of hard X-ray irradiated Xe clusters triggered the development of the 'on-the-fly' connection between *XMDYN* and *XATOM*. It was necessary to address heavy elements for which a precalculation of the atomic data is not feasible owing to a very large number of possible electronic configurations. Typically, this is the case for deeply ionized heavy atoms such as, for example, L-shell-ionized Xe.

Although the original goal of the *XMDYN* development was to address high-intensity phenomena, the tool has also been applied to the single-photon excitation case with remarkable success. The dynamics of C_{60} molecules were followed after a single photoionization event. The predicted electron spectrum and C_{60} molecular ion yield were compared with available experimental data (Jurek *et al.*, 2014). The remarkable agreement between our simulation and experiment confirms that the relevant physics is captured by our model. Though more accurate fully *ab initio* theoretical descriptions of this case are possible, *XMDYN* enables one to predict the system response in a computationally efficient way. Note that in the case of low ionization degree chemical bonds may survive; therefore, they should be treated in the simula-

tions. A rigorous treatment of the bonds in a highly excited environment is not possible at present. In the above examples on C_{60}, we used a classical many-body potential for fullerene (Brenner, 1990), with a phenomenological treatment of bond breaking: the bonding force was set to zero whenever both carbon atoms within a bonded pair were ionized.

XMDYN has also been applied to the field of X-ray imaging, where it is crucial to understand the rapidly progressing radiation damage of the imaged sample. This code is part of the large-scale simulation project *simS2E*, a modular pipeline of computational tools designed for the description of the entire single-molecule imaging process (Yoon *et al.*, 2016; Mancuso *et al.*, 2015).

4. Applicability of the model

The typical X-ray beam parameters currently available at the hard XFEL facilities (Emma *et al.*, 2010; Ishikawa *et al.*, 2012) are a photon energy of $\omega \simeq 0.5$–25 keV, a pulse duration of $T \simeq 1$–100 fs, a pulse energy of $\epsilon \simeq 0.1$–1 mJ on the target and a focal area of $A \simeq 1\ \mu m^2$, which give a range of the peak intensity of $I \simeq \epsilon/(TA) \simeq 10^{17}$–$10^{20}$ W cm^{-2}.

To treat bound electron dynamics, we employ the rate-equation model, tracking populations only and neglecting coherences between population changes. This is justified by the fact that a relatively large bandwidth in ω of an XFEL ($\sim$1%) yields a shorter coherence time than time scales of photoabsorption in the range of I (Son & Santra, 2012). In strong-field physics, laser–matter interaction is characterized by the ponderomotive energy $U_p = I/(4\omega^2)$ in atomic units and the Keldysh parameter $\gamma = [I_p/(2U_p)]^{1/2}$ (Sheehy & DiMauro, 1996), where I_p is the ionization potential of the system. Even at high peak intensity, U_p remains small because of the high ω, and $U_p \ll I_p$ is typically satisfied in the hard X-ray regime. For $\gamma > 1$, neither over-the-barrier nor tunneling ionization can occur.

To treat dynamics of ions and free electrons, we employ the classical model of real-space dynamics. The electromagnetic field drives an oscillatory motion of the charged particles, but the classical amplitude of this motion ($\propto I^{1/2}/\omega^2$) is negligible in the hard X-ray regime. The adequacy of the classical model is quantified in plasma physics by $\Theta \propto E_T/n^{2/3}$ (Murillo & Weisheit, 1998), where E_T is the thermal energy and n is the plasma electron density. Classical description is adequate if $\Theta > 1$, expressing that the plasma is nondegenerate. Further testing of the classical approach is based on the comparison of the de Broglie wavelength of the electron λ with the ion–ion distances d. For $\lambda \ll d$, we can neglect quantum effects such as multiple scattering.

Under the intense irradiation of an XFEL beam the above conditions are usually fulfilled. Nevertheless, post-validation of classicality using the *XMDYN* output of the dynamics is recommended.

5. Program architecture and supported platforms

5.1. *XATOM*

XATOM is mainly written in Fortran 90. Some routines are written in Fortran 77. *XATOM* is compiled with the Intel Fortran Compiler (12.1.5) and Math Kernel Library, on the Scientific Linux System (2.6.18).

5.2. *XMDYN*

XMDYN is written in the programming language C. It is designed for Unix-like environments and has been tested on Linux platforms. GPU extensions are written in nvidia's CUDA language (http://www.nvidia.com/cuda).

6. Usage

6.1. *XATOM*

In order to run *XATOM*, one needs to specify an atomic species (`-system` or `-s`) and an electronic configuration (`-config`). Alternatively, one may specify a hole configuration (`-hole`) instead of the electronic configuration. If the electron/hole configuration is not specified, then the ground-state configuration of the neutral atom is used.

```
./xatom -s Ne
./xatom -s Ne -config 1s1_2s2_2p6
./xatom -s Ne -hole 1s1
```

The output shows computational parameters and orbital energies, which are easily readable with proper descriptions and units.

In order to calculate photoionization cross sections, one needs to use the option `-pcs` and to specify a photon energy (`-photon_energy` or `-PE`). For example, the photoionization cross section of Ne at a photon energy of 2 keV is calculated as below.

```
./xatom -s Ne -pcs -PE 2000
```

Auger decay rates are calculated with `-auger` and fluorescence rates with `-fluorescence`, or both rates are calculated with `-decay`. To calculate the rates of these decay processes, one needs an input configuration with at least one core vacancy using `-config` or `-hole`.

```
./xatom -s Ne -hole 1s1 -decay
./xatom -s Ne -hole 1s1 -auger
./xatom -s Ne -hole 1s1 -fluorescence
```

All outputs are in an easily readable format with descriptions and units.

All of the command-line options mentioned above can be integrated into an input file. One can simply run an example

```
./xatom Ne.in
```

which contains the following lines:

```
system= Ne
config= 1s1_2s2_2p6
photon_energy= 2000
pcs= yes
decay= yes
```

XATOM then calculates orbital energies, photoionization cross sections at 2 keV, Auger rates and fluorescence rates of the single-core-hole state of Ne.

In order to communicate with *XMDYN*, the option of `-xmdyn` must be used. The calculated atomic data in a format compatible with *XMDYN* are printed to the standard output.

One can suppress other outputs except the *XMDYN* format with `-silent`. The output with `-xmdyn` and `-silent` is typically transferred into the input of *XMDYN* *via* a pipeline within the operating system.

6.2. *XMDYN*

XMDYN can be run from the command line by specifying an address folder as a command-line argument. The folder contains input files prepared by the user and output files saved during the run. The input consists of a subfolder `sample`, with files describing the sample, and of an input file `input.txt`. Typically two files should be available in the subfolder `sample` to define a system of N atoms: `Z.txt` containing the respective atomic numbers as a list of N ASCII numbers and `r.txt` containing the initial atomic coordinates as an $N \times 3$ size ASCII matrix. The file `input.txt` lists the parameters of the X-ray pulse (*e.g.* photon energy, pulse duration *etc.*) and parameters of the algorithms (*e.g.* integrator, timestep *etc.*). It may contain various options to control simulated processes (*e.g.* to switch on/off real-space propagation, photoionization or sample-specific force fields, to change the Coulomb force regularization parameter *etc.*) and miscellaneous parameters (*e.g.* snapshots numbers *etc.*). A typical input file (with a few options commented out, switching on/off blocks or processes) looks like this:

```
############################################################
###### A minimalistic XMDYN input file for 1ps propagation

### Propagation, snapshots
DT              1e-18           # timestep [s]
STEPS           1000000         # number of timesteps
SNP             90000:1000:110000,150000:50000:
PROGRESS        1000            # progress logging

### MD integrator and its parameters
MD_INTEGRATOR   verlet

### X-ray pulse parameters
EPH             485             # photon energy [eV]
NPH             1e+10           # fluence [1/(micrometre)^2]
T               10e-15          # pulse duration [s]
T0              100e-15         # center of beam in time [s]
PROFILE         gaussian        # temporal pulse profile:
                                # step or gaussian
### Blocks, processes on/off (y/n)
#md              n              # MD-block on/off
#ph              n              # photoionization on/off
#fl              n              # fluorescent decay on/off
#au              n              # Auger decay on/off
#si              n              # secondary ionization on/off
#re              n              # recombination on/off

############################################################
```

The output files are in text format. The snapshots are collected in separate subfolders named after the timestep within the folder `snp`. In a snapshot folder, the corresponding files containing coordinates, velocities and charges of the particles and the electronic configuration of the atoms/ions can be found. Scattering data may also be saved in these folders, if indicated in the input file. In the top-level folder other text files are created such as `events.log` and `progress.log`. They contain information on all events that occurred during the run and about the progress of the run.

7. Outlook

Both *XATOM* and *XMDYN* are under development. Currently, *XATOM* is being extended to the molecular case (Hao *et al.*, 2015). Furthermore, a relativistic extension is being introduced in order to get accurate results for heavy elements (Toyota *et al.*, 2016). *XMDYN* is being extended to model bulk systems using periodic boundary conditions (Abdullah *et al.*, 2016). A two-step scheme joining MD and continuum approaches is under development to address spectroscopy experiments, particularly for large finite samples. *XMDYN* simulates the initial, non-equilibrium phase of the time evolution, when the interaction with the intense X-ray pulse takes place. Later, when the highly excited atomic states have already decayed and the sample has reached thermal equilibrium, a transition is made from the particle to the density picture. The continuum system is then propagated in the second step by the hydrodynamic tool *XHYDRO* (Saxena *et al.*, 2015) with high efficiency. These methodological developments enable many new applications in the blooming field of XFEL science.

8. Documentation and availability

A downloadable version of the *XATOM* and *XMDYN* tools is available for external users through a free licensing procedure. For further information, please visit http://www.desy.de/~xraypac.

Acknowledgements

The authors thank the users Malik M. Abdullah, Otfried Geffert, Vikrant Saxena, Jan Malte Slowik, Robert Thiele and Koudai Toyota for testing the codes and for the constructive feedback during their development.

References

Abdullah, M. M., Jurek, Z., Son, S.-K. & Santra, R. (2016). Submitted.
Ackermann, W. *et al.* (2007). *Nat. Photon.* **1**, 336–342.
Barash, D., Yang, L., Qian, X. & Schlick, T. (2003). *J. Comput. Chem.* **24**, 77–88.
Brenner, D. W. (1990). *Phys. Rev. B*, **42**, 9458–9471.
Ditmire, T. (1998). *Phys. Rev. A*, **57**, R4094–R4097.
Doumy, G. *et al.* (2011). *Phys. Rev. Lett.* **106**, 083002.
Emma, P. *et al.* (2010). *Nat. Photon.* **4**, 641–647.
Fukuzawa, H. *et al.* (2013). *Phys. Rev. Lett.* **110**, 173005.
Galli, L., Son, S.-K., Barends, T. R. M. *et al.* (2015). *IUCrJ*, **2**, 627–634.
Galli, L., Son, S.-K., Klinge, M. *et al.* (2015). *Struct. Dyn.* **2**, 041703.
Galli, L., Son, S.-K., White, T. A., Santra, R., Chapman, H. N. & Nanao, M. H. (2015). *J. Synchrotron Rad.* **22**, 249–255.
Georgescu, I., Saalmann, U. & Rost, J. M. (2007). *Phys. Rev. A*, **76**, 043203.
Gnodtke, C., Saalmann, U. & Rost, J.-M. (2011). *New J. Phys.* **13**, 013028.
Hamada, T. & Iitaka, T. (2007). *arXiv*:astro-ph/0703100.
Hao, Y., Inhester, L., Hanasaki, K., Son, S.-K. & Santra, R. (2015). *Struct. Dyn.* **2**, 041707.
Hau-Riege, S. P., London, R. A. & Szoke, A. (2004). *Phys. Rev. E*, **69**, 051906.
Hau-Riege, S. P., Weisheit, J., Castor, J. I., London, R. A., Scott, H. & Richards, D. F. (2013). *New J. Phys.* **15**, 015011.
Ishikawa, T. *et al.* (2012). *Nat. Photon.* **6**, 540–544.

Jungreuthmayer, C., Geissler, M., Zanghellini, J. & Brabec, T. (2004). *Phys. Rev. Lett.* **92**, 133401.
Jurek, Z., Faigel, G. & Tegze, M. (2004). *Eur. Phys. J. D*, **29**, 217–229.
Jurek, Z., Santra, R., Son, S.-K. & Ziaja, B. (2016). *XRAYPAC – a Software Package for Modeling X-ray-Induced Dynamics of Matter*. Version 1.0. CFEL, DESY, Hamburg, Germany. http://www.desy.de/~xraypac/.
Jurek, Z., Ziaja, B. & Santra, R. (2013). *XMDYN*. CFEL, DESY, Hamburg, Germany.
Jurek, Z., Ziaja, B. & Santra, R. (2014). *J. Phys. B At. Mol. Opt. Phys.* **47**, 124036.
Kim, Y.-K. & Rudd, M. E. (1994). *Phys. Rev. A*, **50**, 3954–3967.
Makris, M. G., Lambropoulos, P. & Mihelič, A. (2009). *Phys. Rev. Lett.* **102**, 033002.
Mancuso, A. *et al.* (2015). *Start-to-End Simulations (simS2E)*, http://www.xfel.eu/sims2e.
Motomura, K. *et al.* (2013). *J. Phys. B At. Mol. Opt. Phys.* **46**, 164024.
Murillo, M. S. (1998). *Phys. Rep.* **302**, 1–65.
Murphy, B. F. *et al.* (2014). *Nat. Commun.* **5**, 4281.
Peltz, C., Varin, C., Brabec, T. & Fennel, T. (2012). *New J. Phys.* **14**, 065011.
Qian, X. & Schlick, T. (2002). *J. Chem. Phys.* **116**, 5971–5983.
Rohringer, N. & Santra, R. (2007). *Phys. Rev. A*, **76**, 033416.
Rudek, B., Rolles, D. *et al.* (2013). *Phys. Rev. A*, **87**, 023413.
Rudek, B., Son, S.-K. *et al.* (2012). *Nat. Photon.* **6**, 858–865.
Santra, R. (2009). *J. Phys. B At. Mol. Opt. Phys.* **42**, 023001.
Santra, R. & Young, L. (2014). In *Synchrotron Light Sources and Free-Electron Lasers*, edited by E. Jaeschke, S. Khan, J. R. Schneider & J. B. Hastings. Switzerland: Springer.
Saxena, V., Jurek, Z., Ziaja, B. & Santra, R. (2015). *High Energ. Density Phys.* **15**, 93–98.
Sheehy, B. & DiMauro, L. F. (1996). *Annu. Rev. Phys. Chem.* **47**, 463–494.
Siedschlag, C. & Rost, J. M. (2002). *Phys. Rev. Lett.* **89**, 173401.
Slater, J. C. (1951). *Phys. Rev.* **81**, 385–390.
Slowik, J. M., Son, S.-K., Dixit, G., Jurek, Z. & Santra, R. (2014). *New J. Phys.* **16**, 073042.
Son, S.-K., Chapman, H. N. & Santra, R. (2011). *Phys. Rev. Lett.* **107**, 218102.
Son, S.-K., Chapman, H. N. & Santra, R. (2013). *J. Phys. B At. Mol. Opt. Phys.* **46**, 164015.
Son, S.-K. & Santra, R. (2011). *XATOM*. CFEL, DESY, Hamburg, Germany.
Son, S.-K. & Santra, R. (2012). *Phys. Rev. A*, **85**, 063415.
Son, S.-K., Thiele, R., Jurek, Z., Ziaja, B. & Santra, R. (2014). *Phys. Rev. X*, **4**, 031004.
Son, S.-K., Young, L. & Santra, R. (2011). *Phys. Rev. A*, **83**, 033402.
Swope, W. C. (1982). *J. Chem. Phys.* **76**, 637–649.
Tachibana, T. *et al.* (2015). *Sci. Rep.* **5**, 10977.
Thiele, R., Son, S.-K., Ziaja, B. & Santra, R. (2012). *Phys. Rev. A*, **86**, 033411.
Tong, X. M. & Chu, S. I. (1997). *Chem. Phys.* **217**, 119–130.
Toyota, K., Son, S.-K. & Santra, R. (2016). In preparation.
Yao, G. H. & Chu, S. I. (1993). *Chem. Phys. Lett.* **204**, 381–388.
Yoon, C. H. *et al.* (2016). *Sci Rep.* **6**, 24791.
Young, L. *et al.* (2010). *Nature*, **466**, 56–61.
Ziaja, B., de Castro, A. R. B., Weckert, E. & Möller, T. (2006). *Eur. Phys. J. D*, **40**, 465–480.